IEEE Access
Multidisciplinary | Rapid Review | Open Access Journal

Received May 9, 2022, accepted May 20, 2022, date of publication May 25, 2022, date of current version June 2, 2022.

*Digital Object Identifier 10.1109/ACCESS.2022.3177732*

# Measurement and Simulation-Based Exposure Assessment at a Far-Field for a Multitechnology Cellular Site up to 5G NR

**MOHAMMED S. ELBASHEIR[1], RASHID A. SAEED[2], AND SALAHELDIN EDAM[1]**
[1]School of Electronics Engineering, College of Engineering, Sudan University of Science and Technology, Khartoum 14413, Sudan
[2]Department of Computer Engineering, College of Computers and Information Technology, Taif University, Taif 21944, Saudi Arabia

Corresponding author: Mohammed S. Elbasheir (mohd.suleiman@gmail.com)

**ABSTRACT** 5G is expected to be the dominant technology for mobile networks in the coming years, but there is concern about the increase in the total electromagnetic field radiation levels due to the deployment of the 5G technology. This paper presents an exposure assessment of electromagnetic field radiation on humans from single base station of a mobile network serving in dense, urban, suburban, and rural area scenarios for single-site transmission with multi-technology, including 2G, 3G, 4G, IoT, and 5G which have recently been deployed. This assessment is performed using simulation to predict the received signal levels and to calculate the related power densities for a typical single site under operating field configurations and settings for each technology. Field measurements were performed using a drive test tool to validate and calibrate the simulation results. The results show the total exposure ratio was very low compared to the international standard exposure limits, and the results show the contribution from each technology for these spesfic sites used in this study.

**INDEX TERMS** 5G, EMF radiation, exposure assessment, power density, total exposure ratio.

## I. INTRODUCTION

Rapid development is ongoing in mobile networks, causing a consequent increase in the number of transmitting base stations (BS) inside and outside populated towns and cities. An immense number of BSs has been installed to increase network capacity and coverage using various type of sites (macro, micro, and femto). In 5G, there is a huge demand for wireless and internet services, which increases the number of mobile subscribers and customer premises equipment (CPE). This will lead to high data transmission over mobile networks by 2030 compared to 2020 [1], [2]. As a result of the great progress in network technology and solutions, most of the deployed sites involve 2G, 3G, 4G, and recently 5G with the Internet of Things (IoT). This raises questions about the health effects on the human side due to the expected increase in electromagnetic field (EMF) radiation levels with the recent addition of newly deployed systems and technologies, including related BSs and handset devices [3].

Reliable international organizations have adopted and issued standard guidelines, the Federal Communication Commission (FCC) in USA [6], and the ICNIRP standard (International Commission on Non-Ionizing Radiation Protection) which is the most important [4], [5] and is used by regulators in many countries around the world to control the installation and operation of those BSs. The ICNIRP guidelines differentiate between occupationally exposed individuals and members of the general public. Occupationally-exposed individuals are defined as adults who are exposed under controlled conditions associated with their occupational duties, trained to be aware of potential radiofrequency EMF risks and to employ appropriate harm-mitigation measures, and who have the sensory and behavioral capacity for such awareness and harmmitigation response. The general public is defined as individuals of all ages and of differing health statuses, which includes more vulnerable groups or individuals, and who may have no knowledge of or control over their exposure to EMFs [4].

It is anticipated that 5G technology will be the system of general purposes [7] that provides high capacity and enables many features and services that create more business development into worldwide economic production. This requires building 5G networks and installing their BSs either as stand-alone (SA) or non-stand-alone (NSA) as co-located with existing technology 2G/3G/4G/IoT. This massive technology at one site may lead to an increase in

The associate editor coordinating the review of this manuscript and approving it for publication was Gerardo Di Martino.

RF radiation that needs to be studied to quantify and assess the overall radiation level from multi-technology sites in the near field and at the far-field to verify the levels vs standard limits. In this work, as an objective, we used a real mobile network BS site operating with typical configurations in a real environment to study and assess the exposure levels at the far-field for the general public. The assessment was performed using measurement and simulation calculations considering four scenarios: sites in dense, urban, suburban, and rural areas.

The motivation of this study is the importance of having a systematic approach for assessing the EMF exposure levels from multiple wireless technologies at the same site. Our research question is whether there is a probability of the EMF radiation rising above the standard limits if the BS is deployed with multiple technologies. The study also needs to look at other work result indications and benchmarks with related work, which opens doors for further investigations to study overall exposure and correlate it with network design for deploying new solutions such as 5G and future technologies [8], [9]. Of note, in the future (in the next step), we plan to study and assess the exposure level in the near field, which is mainly the interest of occupational workers. Also, we would like to remind that the intention of this study is not to compare the exposure for 2G to 4G vs 5G, the intention is to find the accumulated far-field exposure level when all these technologies are present in a single site.

Many related studies have recently investigated EMF exposure assessment [10], [11]. Some studies used field measurements and others used simulation (calculations). Both methods have focused on single technology assessment (2G, 3G, 4G, IoT, or 5G), and recently there is some focus given on accumulated exposure from multi-technology coexisting at a single site, and few studies investigated this subject [37] which we believe is important to address. More factors need to be considered and require further investigation, such as the co-location of the multi-operator situation at the same site, accumulated radiation from neighboring and surrounding sites, actual radiation considering the number of users, traffic load (system utilization), and especially for 5G NR, the time-averaged power and spectral efficiency [38], [39].

The novelty of this study is to provide RF-EMF exposure radiation assessment for a typical single site in dense, urban, suburban, and rural areas considering multi-technology (including 2G, 3G, 4G, IoT, and 5G) simultaneously operating and co-located at the same site.

This paper is structurally organized into three sections: the site description and methodologies used in the simulations and assessment, the limits of the ICNIRP standards, and the output results with related analysis from different perspectives, signal level, power density, and total exposure.

## II. ASSESSMENT MODEL AND SITE DESCRIPTION

### A. ASSESSMENT PROCESS

In this study, a set of related activities are performed according to the process flow as shown in FIGURE 1.

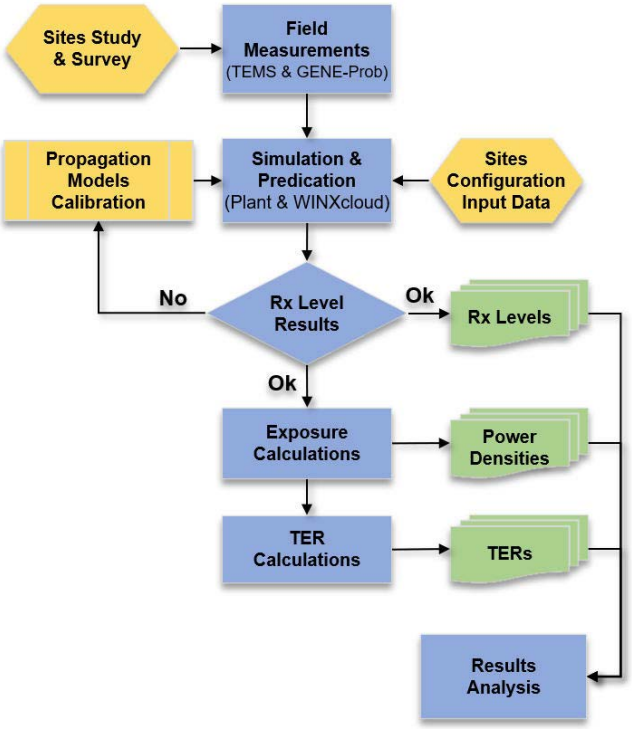


**FIGURE 1.** The process used for EMF exposure assessment.

Field measurements were collected for selected sites, and the results were used to calibrate the simulation tool propagation model to achieve higher accuracy by fine-tuning the propagation model parameters and correction factor, both of which depend on the environment type. The simulation was performed to predict the Rx signal levels of each technology for selected sites. Using the predicted Rx level results for each technology (2G, 3G, 4G, IoT, and 5G), the exposure level emitted from each technology is calculated in terms of power densities, which are used as input to calculate the total exposure ratio (TER) and to analyze its related characteristics and behavior for different scenarios.

### B. SITE DESCRIPTION

Real network sites belonging to one operator in the Kingdom of Saudi Arabia (KSA) are used in this study, and all sites include multi-technology 2G/3G/4G/IoT/5G coexisting in the same site tower, and all are on-air in service at the same time. The used site configurations and related data are typical for the current operating network that provides actual results based on the actual setup, and this was our main purpose for using live network data. Of course, other networks might have different settings, which may lead to different results. To enrich this study, four sites were selected to represent four assessment scenarios. Site-1 is located in a dense area in the downtown of Dammam city in the eastern region, this site services dense commercial and residential areas. The antennas of all technologies are installed on the building rooftop at 20 m height from ground level. MAP 1 shows the


**Map 1.** The geographical location of site-1 in the dense area.

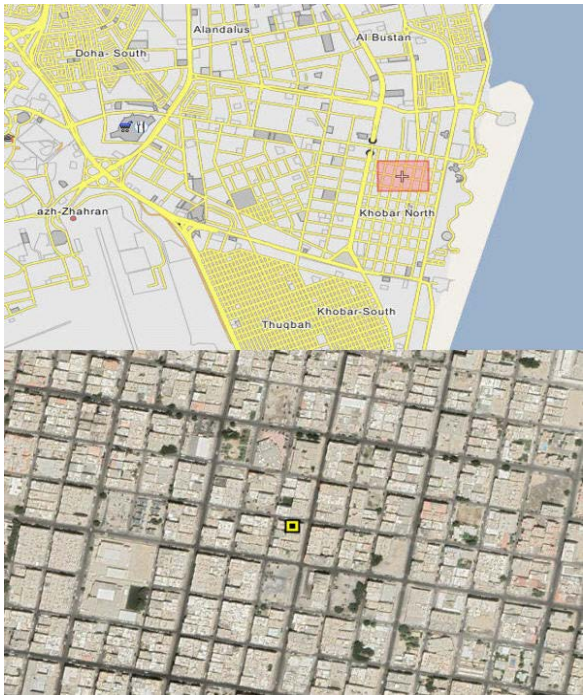


**Map 2.** The geographical location of site-2 in the urban area.


**Map 3.** The geographical location of site-3 in the suburban area.

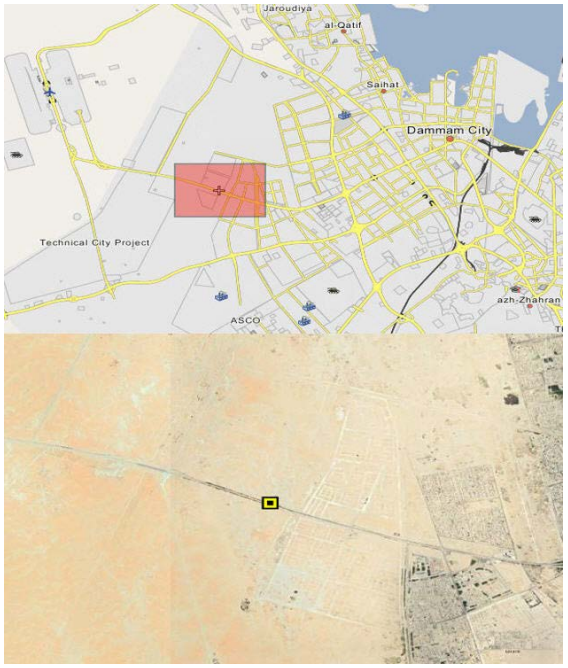


**Map 4.** The geographical location of site-4 in the rural area.

site location on the Google Earth map, and Table 1 shows the site data and operating configurations.

Site-2 is located in an urban area in Khubar city in the eastern region. This site services mainly residential areas with some commercial area near the Arbian Gulf coast, and the antennas of all technologies are installed on the building rooftop at 25 m height from ground level. MAP 2 shows the site location on the Google Earth map, and Table 1 shows the site data and operating configurations.

Site-3 is located in a suburban area in Dhahran city (in the eastern region of the KSA), which is a purely residential area. The antennas of all technologies were installed on the greenfield monopole tower at a height of 30 m from the ground level. MAP 3 shows the site location on the Google

**TABLE 1. Configuration setup of the selected sites.**

| Site Setting | 2G G900 | 3G U900 | 4G L800 | 4G L1800 | 4G L2100 | 5G NR2600 |
|---|---|---|---|---|---|---|
| Freq. Band (MHz) | 900 | 900 | 800 | 1800 | 2100 | 2600 |
| Freq. BW (MHz) | 400 | 4.2 | 10 | 10 | 20 | 60 |
| Number of Tx | 2T | 1T | 2T | 2T | 4T | 64T |
| Number of Rx | 2R | 2R | 2R | 4R | 4R | 64R |
| Total Tx Power (Watt) | 40 | 40 | 80 | 40 | 40 | 96 |
| System Utilization | 95% | 95% | 95% | 95% | 95% | 95% |
| Ant. Gain (dBi) | 17 | 17 | 16.7 | 16.6 | 17 | 24.8 |
| Horizontal BW | 60° | 60° | 65° | 65° | 65° | 65° |
| Vertical BW | 7.5° | 7.5° | 7.8° | 6° | 6° | 6.5° |
| Ant. Tilt Angle | -6° | -6° | -6° | -6° | -6° | -6° |
| Ant. Height Dense | 20 m | 20 m | 20 m | 20 m | 20 m | 20 m |
| Ant. Height Urban | 25 m | 25 m | 25 m | 25 m | 25 m | 25 m |
| Ant. Height Sub-Urban | 30 m | 30 m | 30 m | 30 m | 30 m | 30 m |
| Ant. Height Rural | 60 m | 60 m | 60 m | 60 m | 60 m | 60 m |

Earth map, and Table 1 shows the site data and operating configurations.

Site 4 is located in a rural area on the highway to Dammam International Airport, which is located 30 km from Dammam city. This site services highway roads and is under the construction of new residential areas. The antennas of all technologies were installed on the greenfield tower at a 60 m height from the ground level. MAP 4 shows the site location on the Google Earth map, and Table 1 shows the site data and operating configurations.

### C. SITE CONFIGURATIONS SETUP

In this study, the same configurations and setups were used for the four sites, including Tx/Rx hardware, equipment types, antenna gain, bandwidth, frequency ranges, and transmitting power. Except for the antenna heights, the antennas were installed at different heights in each scenario. These are the actual on-air operating configurations, and this was intentionally considered in this study to evaluate the radiation emissions based on actual scenarios. At each site, 3-sector BTS (base transceiver station) is installed per technology, and antenna azimuths were horizontally directed with a 120-degree spacing between every two sectors (each sector cover 120 degree).

At the four sites, the 2G GSM 900 MHz and 3G UMTS 900 MHz were transmitted from the same radio remote unit (RRU) that was connected to the crossed-polarized antenna by a coaxial feeder. The RRU is connected down through the common public radio interface (CPRI) front-backhaul to the base-band unit (BBU) that handles and controls radio processing, as illustrated in FIGURE 2. The RRU power was spilled between the GSM and UMTS, and the final configuration setup is shown in TABLE 1.

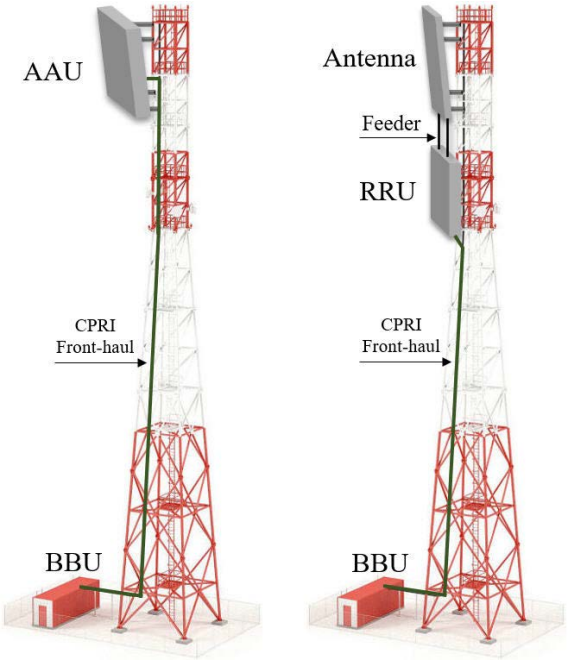


**FIGURE 2. Connectivity setup of the radio remote unit (RRU) used for 2G/3G/4G and the active antenna unit (AAU) used for 5G.**

Similar to the 4G LTE 1800 MHz 2100 MHz, both were transmitted from the same RRU, which was also connected to the crossed polarized antenna by a coaxial feeder, and the RRU power was spilled between both. The 4G LTE 800 MHz was installed in a separate RRU connected to a separate antenna.

The 5G NR 2.6 GHz were transmitted from the massive-MIMO 64T/64R active antenna unit (AAU), which is a physical hardware unit consisting of an integrated radio unit with an antenna. Most technology vendors designed the AAU as a compact practical solution instead of using a large number of antennas, such as the 64 antennas required to transmit the 64T/64R massive-MIMO.

### D. NB-IOT CONFIGURATION

The narrow band IoT (NB-IoT) allows access to network services via LTE [12] with a bandwidth-limited channel to a maximum of 200 kHz [13]. The investigated sites in this study transmitted NB-IoT at 800 MHz with a one-channel 180 kHz bandwidth that consists of 12 subcarriers each at 15 kHz and has the same LTE frame structure as one radio physical resource block (PRB). The NB-IoT is transmitted from the same 2T/2R RRU hardware used by the 4G FDD LTE 800 MHz and connected to one antenna with a 17.6 dBi gain. The total power (80 W) of this IoT/FDD RRU is equally distributed over a total of 50 PRBs (one PRB for IoT, and 49 PRBs for FDD).

### E. FIELD MEASUREMENTS

Field measurements were conducted using two types of drive test tools in different fixed locations around the four selected sites. The first tool is the Test of Mobile System (TEMS®)

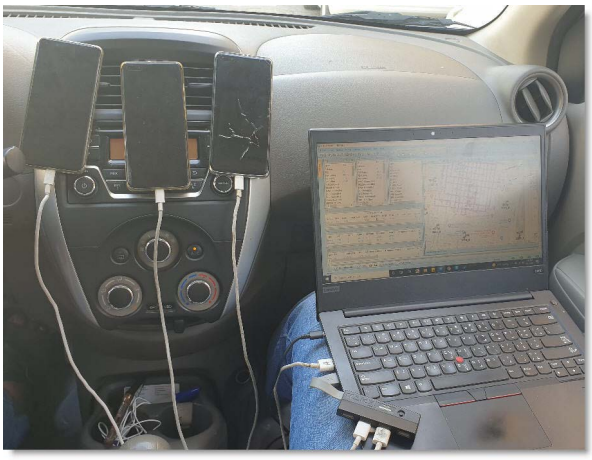

**FIGURE 3.** Photo of the car drive test tool used for field measurements.

Investigation v20 [14], and the second tool is the Huawei GENE-Prob-5. Both tools have software installed on a laptop PC and connected to three mobile user equipment (UE) and GPS antenna, and all were mounted inside a car in front of the dashboard at 1.3-1.5 m height, as shown in FIGURE 3. The tool collects the Rx signal levels from the 3 UEs for one technology at the same time (average results from 3 UEs are used later as input to calibrate the simulation tool). The measurements are recorded in log files with related time and GPS coordinates, and the measured samples were collected every 0.5 s for each UE with more than 2,500 measurement samples for each technology at each fixed location. The measurements were collected in fixed places located at different distances and covered the coverage area of the site. The collected measurement for 2G GSM900 includes the Rx level in dBm of the broadcast common control channel (BCCH), and for 3G UMTS900 includes the received signal code power (RSCP) levels in dBm. The 4G FDD LTE includes the reference signal received power (RSRP) levels in dBm. 5G includes Secondary Synchronization Reference Signal Received Power (SS-RSRP) levels in dBm.

### F. RX LEVELS SIMULATION

Mobile wireless networks require proper radio planning and design for the required capacity and coverage [15]. This should be performed before implementation to ensure that the planned signal levels reach and cover the targeted areas well. A wide variety of approaches have been developed to predict the coverage level using propagation models that calculate the transfer of signals from the transmitter to the receiver. Predication software-based tools were developed to run the predicted computational operations using a suitable propagation model equation according to the site and location data input. In this study, the infovista Planet®v7 simulation tool [16] was used to predict the Rx levels for the 2G/3G/4G technologies of the four sites, and the WINXcloud®1.0 simulation tool was used for 5G RX signal prediction. Both tools used input data, as shown in TABLE 1. The tool was installed with area map data, and the tool was set to calculate with 10 m distance every two points (approximately 17,760 calculated points within an area of 1.5 km radius).

For the 2G 900 MHz and 3G UMTS 900 MHz calculations, we used COST231-Hata, which was developed by European Cooperation in Science and Technology (COST) based on the Okumura-Hata model [17], [18]. This model is suitable for the urban environment and can be used for distances up to 30 km between the BS and receiver. The path loss is presented below EQUATION (1), which expresses path loss in dB as

$$L_{COST231Hata} = 33.9\log f_c - 13.82h_{tr} - ah_{re} + (44.9 - 6.55\log h_{tr})\log d + C_m + 46.3 \quad (1)$$

where $Cm$ is a constant and $ah_{re}$ is the correction factor, and both depend on the environment type.

For the 4G LTE FDD (800, 1800, and 2100 MHz), we used the urban macro cellular model (UMa) developed by 3GPP for frequencies from 450 MHz to 6 GHz [19]. It is suitable for Macro sites where the BS height is assumed to be higher than that of the surrounding rooftops. This model has two modes, non-line of sight (NLOS) and LOS path loss, and EQUATIONS (2-3) represent the UMa-LOS.

$$L_{4GUMa} = 22\log(d) + 28 + 20\log(f)\ 10m \le d \le d_b \quad (2)$$

$$L_{4GUMa} = 40\log(d) - 28 + 20\log(f) - 9\left[(d_b)^2 + (h_t - h_r)^2\right] d_b \le d \le 5000m \quad (3)$$

where $d$ is the distance from the BS, $d_b$ is the break point distance, which depends on the height of the antennas ($d_b = 4h_t h_r / \lambda$), and the model assumes an MS height between 1.5 m and 22.5 m.

With the introduction of 5G New Radio (NR), 3GPP has standardized the UMa model for 5G and covers a wider range of frequencies up to 100 GHz, because there is high expectation that 5G NR will also operate at higher frequencies [20]. The 3GPP UMa 5G model [21] has parameters similar to 4G Uma, with more frequency modules to support a higher frequency range, especially for NLOS MUa modes. This model effectively supersedes all previous models [22]. EQUATIONS (4-6) represent the line of sight (LOS) path loss for 5G UMa used in this study to calculate the 5G Rx level.

$$L_{5GUMa} = \begin{cases} PL_1, \&10m \le d \le d_b \\ PL_2, \&d_b \le d \le 5000m \end{cases} \quad (4)$$

$$PL_1 = 28 + 22\log(d) + 20\log(f) \quad (5)$$

$$PL_2 = 28 + 40\log(d) + 20\log(f) - 9\left[(d_b)^2 + (h_t - h_r)^2\right] \quad (6)$$

where $d$ is the distance from the BS, and $d_b$ is the break point distance depending on the height of the antennas ($d_b =$

$4h_t h_r / \lambda$). This 5G-UMa model also assumes a UE height between 1.5 m and 22.5 m.

This study didn't consider the TDD duty cycle for the TDD bands and beamforming gain is assumed in all directions even though only one direction can reach the maximum gain level while the destructive beamforming in other directions in MIMO and massive MIMO systems.

### G. POWER DENSITY CALCULATION

The EMF exposure standard limits are categorized as basic restrictions and reference levels; thus, power density figures are essential for the level of exposure to EMF radiation. In this study, the predicted Rx levels (in dBm) were used to calculate the power density ($S_{inc}$) in watts per meter square using EQUATION (7), which simply reflects the concentration of the received power density at the UE considering the UE antenna gain and signal frequency [23].

$$S_{inc} = \frac{4\pi}{\lambda^2 . A_g} . P_{Rx} \tag{7}$$

where λ is the wavelength (m), and $A_g$ is the antenna gain of the UE, and $P_{RX}$ is the signal received level at the UE in dBm. In this study, the antenna gain $A_g$ used was −10 dBi [23] for 2.6 to 3.7 GHz, −6 dBi for 900, and −9 dBi for 1800 MHz [24].

In this study the power density for 4G and 5G is calculated using the reference signal channel SS-RSRP. However, only a small fraction of power is transmitted through such channels, while most traffic data is transmitted with PDSCH using different antenna patterns. Thus, the extrapolated power density results do not consider such a difference.

### H. EMF EXPOSURE STANDARD LIMITS

In 1998, the ICNIRP published exposure standards [5], and in 2020, they revised it [4], which included guidelines to limit and control radiation levels to a range of frequencies (100 kHz to 300 GHz) for the general population and occupational workers. The ICNIRP mentions that RF-EMF can affect the human body via two primary biological effects: changes in the permeability of membranes and thermal effects due to temperature increases. Based on massive biological studies, the ICNIRP has defined basic restrictions in terms of the specific absorption rate (SAR) to protect humans from RF adverse health effects. The ICNIRP has put more restrictions and limits on the general population compared to occupational workers.

Because the ICNIRP is the most adopted standard in many countries [25], especially in Europe and the Middle East, in this study, the general public limits are used as a reference for total exposure levels.

From the basic restrictions, a set of reference limits is defined by ICNIRP to translate the radiation restrictions into figures that can be practically measured and applied. Table 2 lists the reference levels; if the radiation is below those levels, it is considered to comply with the standard.

**TABLE 2. ICNIRP reference limits for 0.1 MHz to 300 GHz.**

| Exposure Scenario | Frequency Range | E-filed (V/m) | H-field (A/m) | Power Density ($W/m^2$) |
|---|---|---|---|---|
| Occupational | 0.1-30 MHz | $660/f_M^{0.7}$ | $4.9/f_M$ | *NA* |
| | >30-400 MHz | *61* | *0.16* | *10* |
| | >400-2000 MHz | $3f_M^{0.5}$ | $0.008f_M^{0.5}$ | $f_M/40$ |
| | >2-300 GHz | *NA* | *NA* | *50* |
| General Public | 0.1-30 MHz | $300/f_M^{0.7}$ | $2.2/f_M$ | *NA* |
| | >30-400 MHz | *27.7* | *0.073* | *2* |
| | >400-2000 MHz | $1.375f_M^{0.5}$ | $0.0037f_M^{0.5}$ | $f_M/200$ |
| | >2-300 GHz | *NA* | *NA* | *10* |

In addition, ICNIRP has a defined limit for accumulative exposure of different sources instantaneously radiating, and the total exposure ratio (TER) should be accumulated according to EQUATION (8):

$$TER = \sum_{f=100kHz}^{30\,MHz} \left\{ \left( \frac{E_{inc,f}}{E_{inc,RL,f}} \right)^2 + \left( \frac{H_{inc,f}}{H_{inc,RL,f}} \right)^2 \right\} + \sum_{f>30MHz}^{2GHz} MAX \left\{ \left( \frac{E_{inc,f}}{E_{inc,RL,f}} \right)^2, \left( \frac{H_{inc,f}}{H_{inc,RL,f}} \right)^2, \left( \frac{S_{inc,f}}{S_{inc,RL,f}} \right) \right\} + \sum_{f>2GHz}^{300GHz} \left( \frac{S_{inc,f}}{S_{inc,RL,f}} \right) \leq 1 \tag{8}$$

where $E_{inc,f}$ incident E-field, $H_{inc,i}$ incident H-field, and $S_{inc,f}$ incident power density at frequency f. And, $E_{inc,RL,f}$, $H_{inc,RL,f}$ and $S_{inc,RL,f}$ are incident reference levels of F-field, H-field, and power density at frequency f.

In this study, the TER is evaluated based on power density $S_{inc}$. Accordingly, EQUATION (8) is modified to EQUATION (9)which has been used for all TER calculations.

$$TER = \sum_{f>30MHz}^{300GHz} \left( \frac{S_{inc,f}}{S_{inc,RL,f}} \right) \leq 1 \tag{9}$$

## III. RESULTS AND DISCUSSION

### A. MEASUREMENT RESULTS AND SIMULATION CALIBRATION

The measurement data from the drive test (Rx Levels in dBm at different locations from the sites) were used to calibrate the simulation tool input [26], including the propagation model setup as described and shown in FIGURE 1. The final simulated Rx-Level results for all technologies were compared with the measurement data though point-to-point comparison, and the measurements were found to be lower than the simulated results for all technologies, as shown in FIGURE 4. For example, in 5G NR at 2600 MHz, the average measured SS-RSRP is −78.4 dBm, and the simulated SS-RSRP is −71.6 dBm.

The difference between the measured and simulated values of the final calibrated tool was calculated in terms of the mean error in dB, which reflects the signal loss due to in-car penetration. TABLE 3 shows the mean error for each technology, which indicates that the lowest mean error is

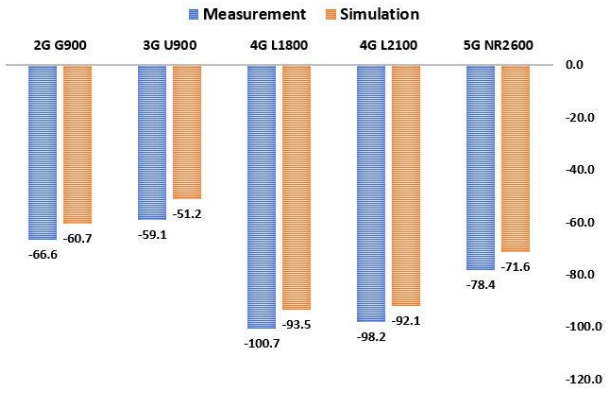


**FIGURE 4.** Measurement vs. simulation for Rx signal levels.

**TABLE 3.** Mean error between measured and simulated signal levels.

| Average Signal Level | 2G G900 | 3G U900 | 4G L1800 | 4G L2100 | 5G NR2600 |
|---|---|---|---|---|---|
| Measurement (dBm) | -66.6 | -59.1 | -100.7 | -98.2 | -78.4 |
| Simulation (dBm) | -60.7 | -51.2 | -93.5 | -92.1 | -71.6 |
| **Mean Error (dB)** | **6.0** | **7.9** | **7.2** | **6.1** | **6.8** |

6.0 dB for 2G GSM 900 MHz, and the highest is 7.2 for 4G LTE 1800 MHz. These results closely match and are in line with the results published in [27], [28].

### B. RX SIGNAL LEVEL PREDICTION RESULTS

The COST231-Hata propagation model of EQUATION (1) is used in the simulation to predict the RX level for the 2G GSM and 3G UMTS at 900 MHz. In addition, the UMa-4G propagation model of EQUATIONS (2-3) is used to predict the 4G LTE FDD (800, 1800, and 2100 MHz) RSRP level, and the UMa-5G propagation model of EQUATIONS (4-6) is used to predict the 5G NR (2.6 and 3.7 GHz) SS-RSRP levels. The calculations were performed for the 4 sites that represent dense-urban, urban, suburban, and rural cases. As an example, FIGURE 5 shows the RSRP level in dBm distribution for 5G NR at 2.6 GHz for the suburban area within a 1.5 km radius from the site.

The mentioned TX power in TABLE 3 is the total power in watt for all transmitters in each technology, for example the 2G G900 has 2 TRXs with a total power of 40 watts (each TRX transmit 20 watts). So, the actual used 5G EIRP (56.6 dBm) is the lowest one and 3G U900 has the highest EIRP (63 dBm. The simulation results of the predicted Rx signal levels were exported and processed to obtain the maximum levels at each 10 m distance step from the site (aggregated for all directions) up to a 1.5-km radius from the site. FIGURE 6 shows the Rx level for all technologies (dBm) for the site in the dense area scenario with the highest strength levels registered from 2G GSM and 3G UMT at 900 MHz and the lowest strength levels recorded from 4G FDD LTE at 1800/2100 MHz.

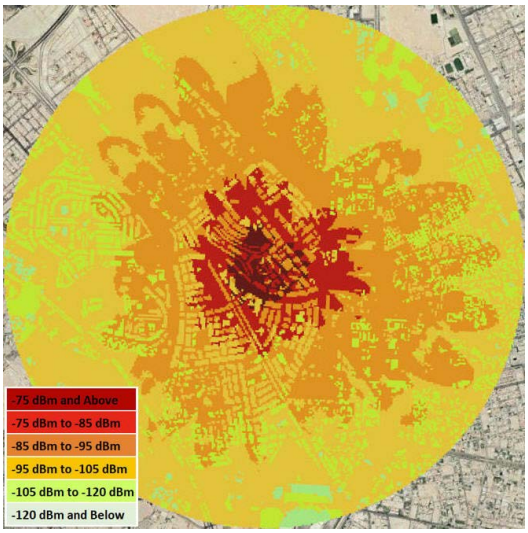


**FIGURE 5.** Site-1 (suburban area) simulated Rx RSRP (dBm) for 5G NR 2600 MHz.

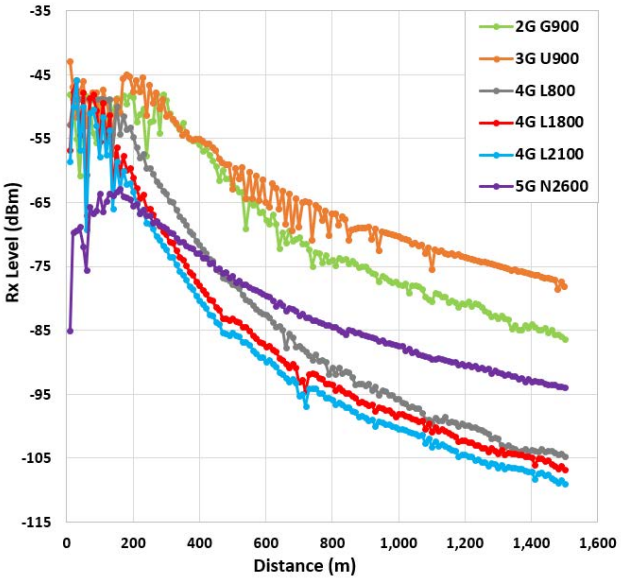


**FIGURE 6.** Site-1 (dense area) simulated Rx level (dBm) for all technologies.

The 5G NR 2.6 GHz results show that signal levels are low in the areas close to the site at a distance of less than 200 m, and the highest signal levels are registered after approximately 200 m. Then, Rx starts to degrade as the distance increases. For distances farther than 200 meters, AAU massive MIMO with beamforming shows good performance in the Rx signal degradation trend compared to 2G/3G/4G, which has a higher signal degradation rate. The simulation results and behaviors were similar for the urban and suburban sites, as shown in FIGURES 7-8. For the rural area site, the Rx levels were calculated for the entire coverage area of up to 6 km, as shown in FIGURE 9. The Rx signal degradation trend with increasing distance was found to be similar to the behavior of dense, urban, and suburban sites.

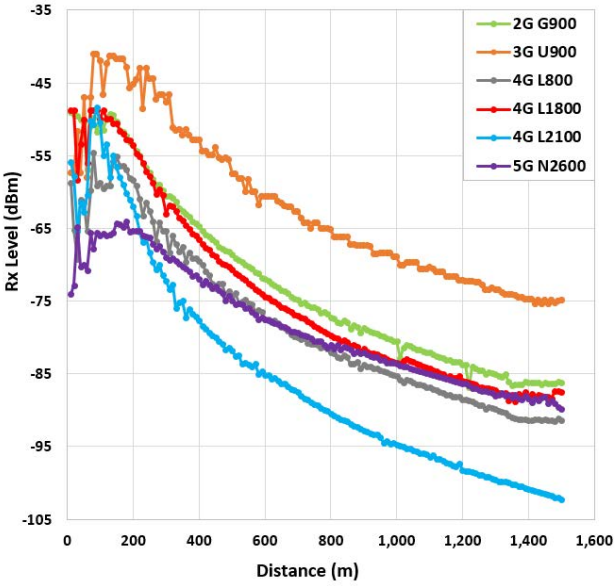


**FIGURE 7.** Site-2 (urban area) simulated Rx level (dBm) for all technologies.

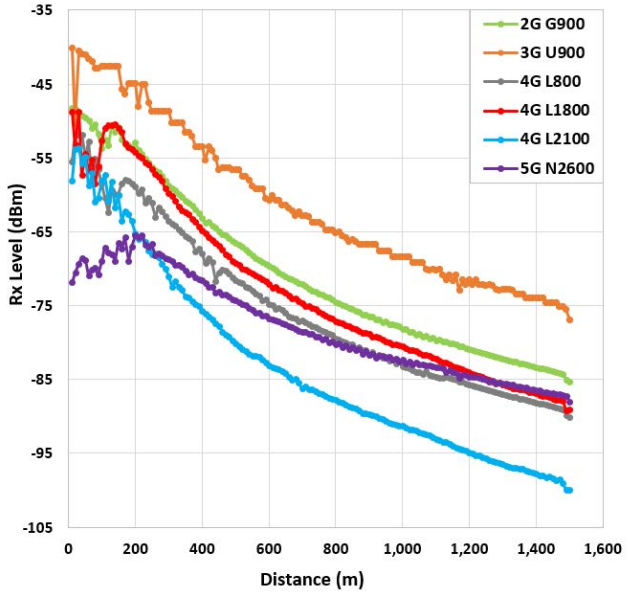


**FIGURE 8.** Site-3 (suburban area) simulated the Rx level (dBm) for all technologies.

The used EIRPs are reflected in the results of Rx level simulation, for example in the dense area site, the RX signal level results show 2G 900 and 3G 900 have higher EIRP compared to 5G 2600 and 4G L800/L1800/L2100. But, the 5G that has massive MIMO with beamforming shows good performance in the Rx signal degradation trend compared to 2G/3G/4G, which has a higher signal degradation rate.

### C. POWER DENSITY RESULTS

EQUATION (7) was used to calculate the total power densities at each point around the site and for all technologies of technology. The predicted Rx levels of the simulation

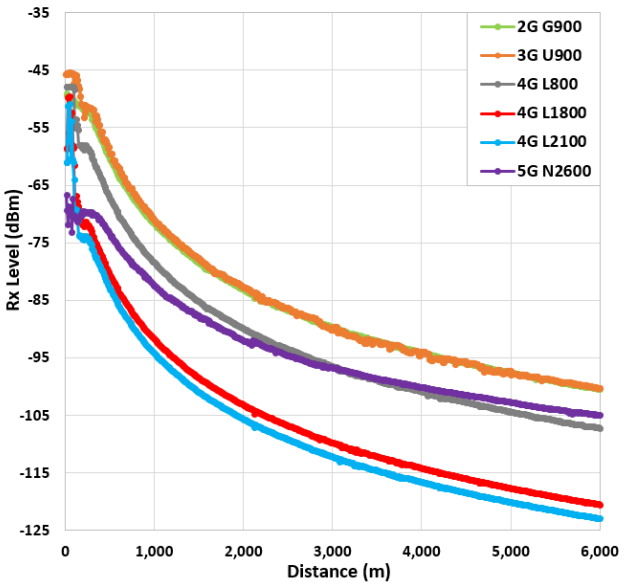


**FIGURE 9.** Site-4 (rural area 6 km) simulated the Rx level (dBm) for all technologies.

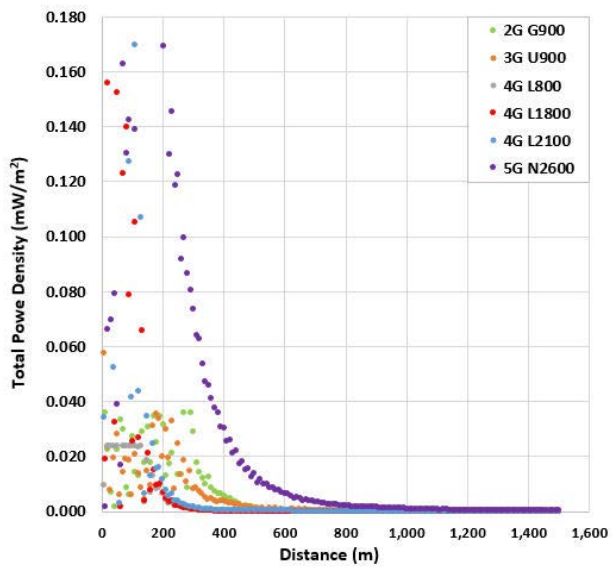


**FIGURE 10.** Site-1 (dense area) simulated the total power density per technology (mW/m$^2$) for all technologies.

results were used as inputs for the power density calculations considering each technology configuration setup, as listed in TABLE 1. The 800 MHz results include the combined power density for both 4G-FDD-LTE and NB-IoT.

For the four scenarios (dense, urban, suburban, and rural), the obtained results show that the power densities from all technologies (2G/3G/4G/5G) are low compared to the reference limit, which is consistent with the results of previously published studies [17], [23], [29]–[36] related to this work.

For the dense area site, as shown in FIGURE 10, the total power densities trend with increasing distance from the site. The evaluation of each technology shows that the

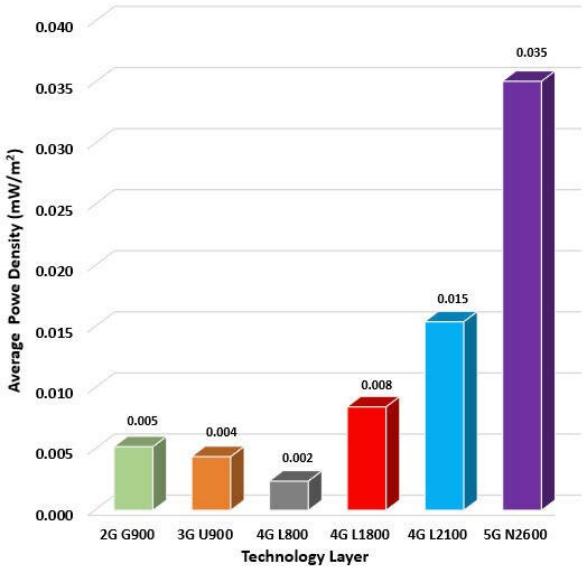


**FIGURE 11.** Site-1 (dense area) the simulated exposure ratios for all technologies.

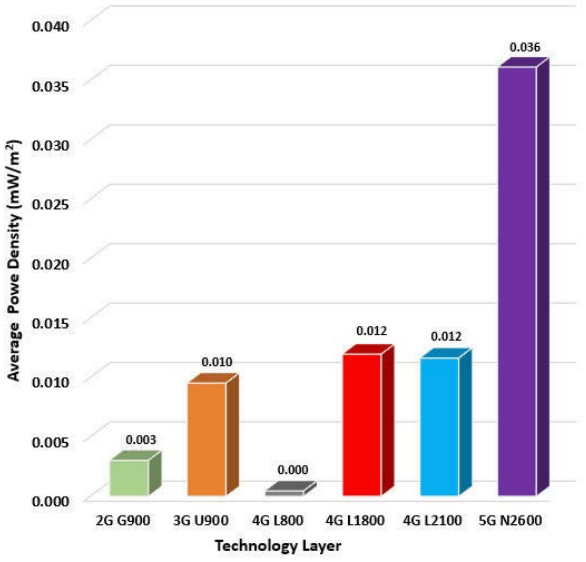


**FIGURE 13.** Site-2 (urban area) the simulated exposure ratios for all technologies.

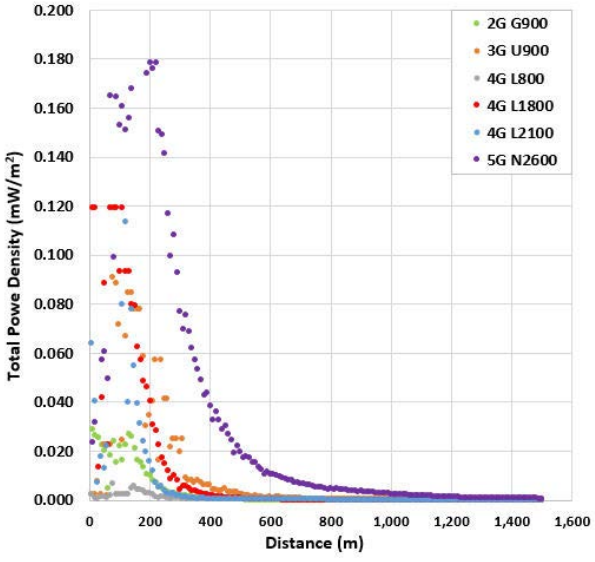


**FIGURE 12.** Site-2 (urban area) simulated the total power density per technology (mW/m$^2$) for all technologies.

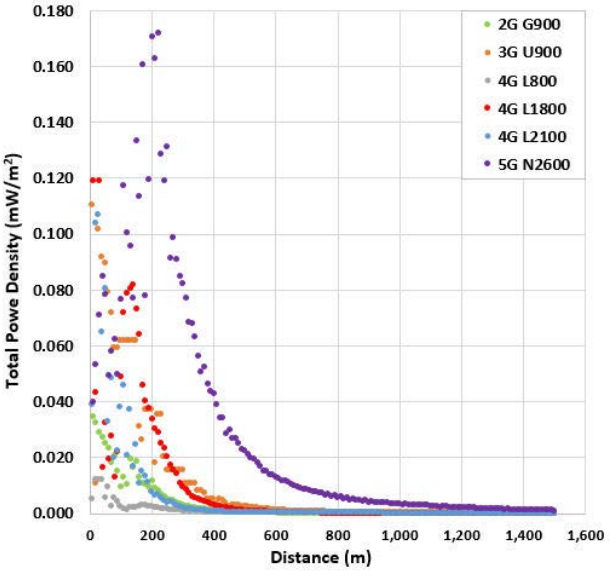


**FIGURE 14.** Site-3 (suburban area) simulated the total power density per technology (mW/m$^2$) for all technologies.

whole average $S_{inc}$ (power density) is recorded as the highest at 35.1 $\mu$W/m$^2$ for 5G, which is 0.0000351% from the ICNIRP reference level of 10 w/m$^2$, and this is only for 5G at 2.6 GHz technology but accumulation with other technologies is calculated using TER. Then, 15.4/8.5 $\mu$W/m$^2$ are recorded for 4G L2100/L1800, 5.2/4.4 $\mu$W/m$^2$ for 2G/3G 900, and 2.4 $\mu$W/m$^2$for IoT/L800, as shown in FIGURE 11. The authors of [40] assessed the RF exposure for GSM900 and GSM1800 at the street level for a larger area using car-mounted measurements, and their results show a power density of 2G G900, which is in line with our simulation results.

For the urban area site, FIGURE 12 shows the total $S_{inc}$ trend with increasing distance, and the evaluation results show that the highest average $S_{inc}$ recorded value is 36.1 $\mu$W/m$^2$ for 5G, 12.0/11.0 $\mu$W/m$^2$ for 4G L1800/L2100, and 9.5/3.0 $\mu$W/m$^2$ for 3G/2G 900, and the lowest $S_{inc}$ is 0.5 $\mu$W/m$^2$for IoT/L800, as shown in FIGURE 13.

For the suburban area site, FIGURE 14 shows the total $S_{inc}$ trend with increasing distance, and the evaluation results show that the highest average $S_{inc}$ recorded value is 29 $\mu$W/m$^2$ for 5G, 9.0/5.5 $\mu$W/m$^2$ for 4G L1800/L2100, and 10.4/3.1 $\mu$W/m$^2$ for 3G/2G 900, and the lowest $S_{inc}$ is 0.8 $\mu$W/m$^2$for IoT/L800, as shown in FIGURE 15.

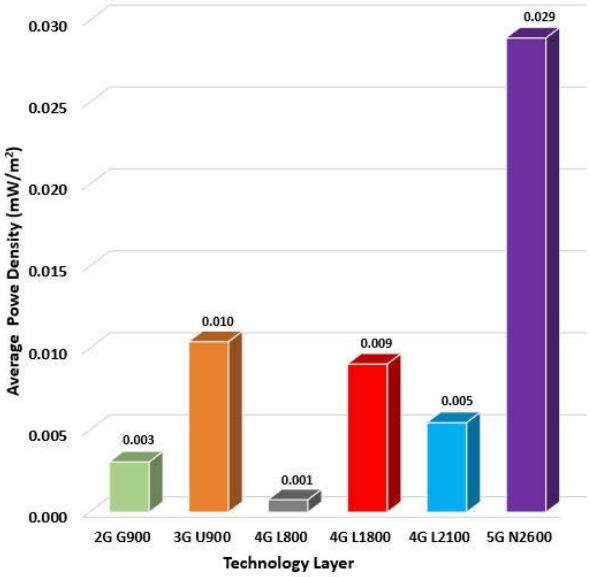


**FIGURE 15.** Site-3 (suburban area) the simulated exposure ratios for all technologies.

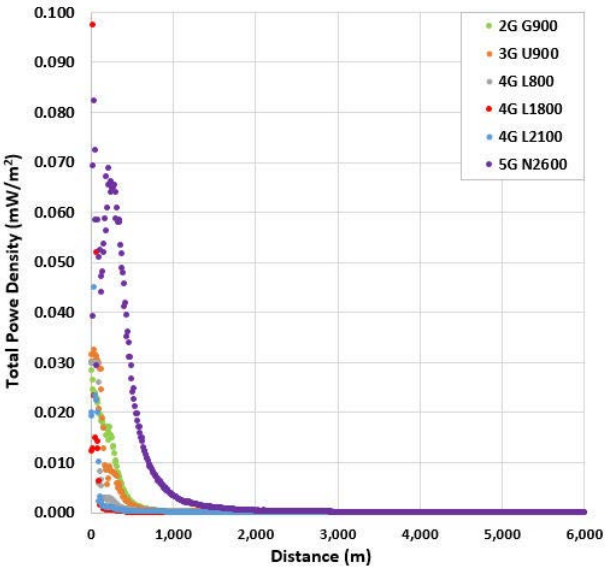


**FIGURE 17.** Site-4 (rural area) simulated the total power density per technology (mW/m$^2$) within 6 km for all technologies.

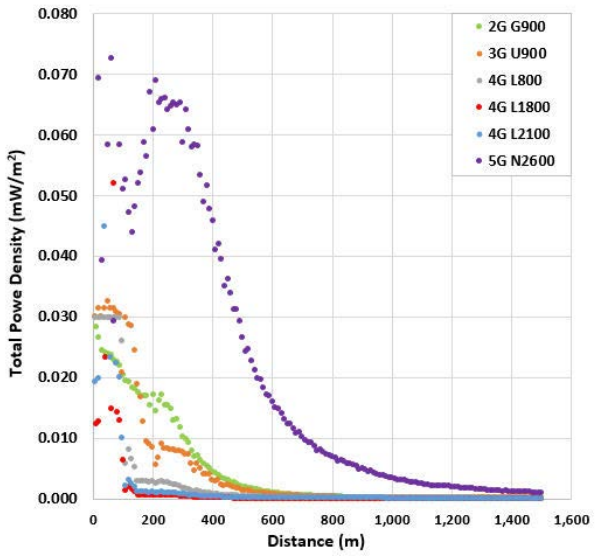


**FIGURE 16.** Site-4 (rural area) simulated the total power density per technology (mW/m$^2$) within 1.5 km for all technologies.

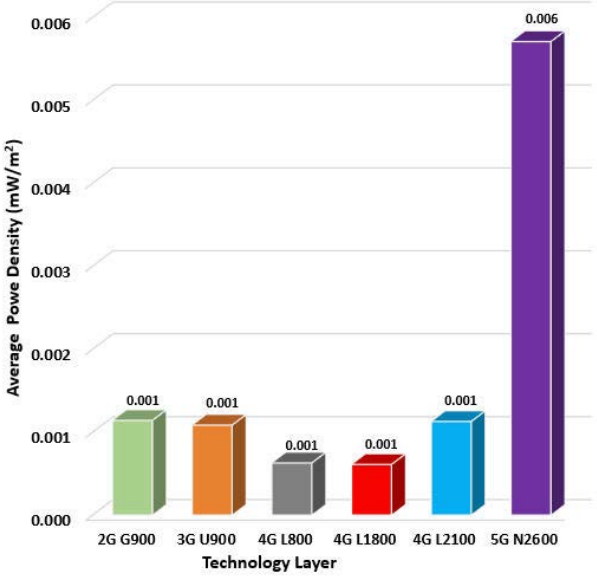


**FIGURE 18.** Site 4 (rural area) the simulated exposure ratios for all technologies.

For the rural area site, the calculated $S_{inc}$ is evaluated for two zones, within 1.5 km (FIGURE 16) and up to 6 km (FIGURE 17), and the evaluation results for 1.5 km show that the highest average $S_{inc}$ recorded value is 22.6 $\mu$W/m$^2$ for 5G, then 4.6/2.5 $\mu$W/m$^2$ for 4G L2100/L1800, and 4.6/4.4 $\mu$W/m$^2$ for 2G/3G 900, and the lowest $S_{inc}$ is 2.5 $\mu$W/m$^2$ for IoT/L800. The evaluation results for 6 km show that the highest average $S_{inc}$ is 5.7 mW/m$^2$ for 5G, then 1.13/0.61 $\mu$W/m$^2$ for 4G L2100/L1800, and 1.14/1.08 $\mu$W/m$^2$ for 2G/3G 900, and the lowest $S_{inc}$ is 0.63 $\mu$W/m$^2$for IoT/L800, as shown in FIGURE 18.

### *D. EXPOSURE RATIO AND TER RESULTS*

Considering that multi-technology coexists and in the same site operating simultaneously and using EQUATIONS (9), the accumulated TER was calculated for the four scenarios, and the simulated power density $S_{inc}$ results with reference limits listed in TABLE 1 were used as inputs for the TER calculations. The obtained results show that the maximum TER is very low compared to the ICNIRP limit, specifically it is $10.5 \times 10^{-5}$ for the dense area, $8.8 \times 10^{-5}$ for the urban area site, $6.2 \times 10^{-5}$ for the suburban area, and $5.6 \times 10^{-5}$ for the rural area. These results are in agreement with the studies published in [17], [23], [29]–[36]. Of note, these studies were

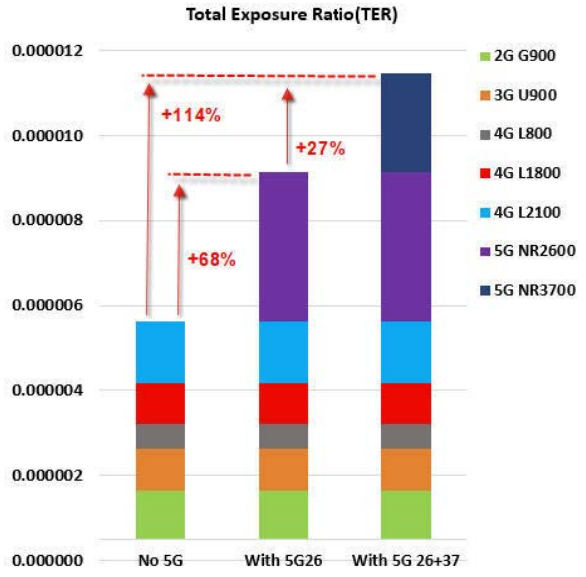


**FIGURE 19.** Site-1 (dense area) simulated increments in the total exposure ratio TER due to the addition of 5G2600 and 5G3700.

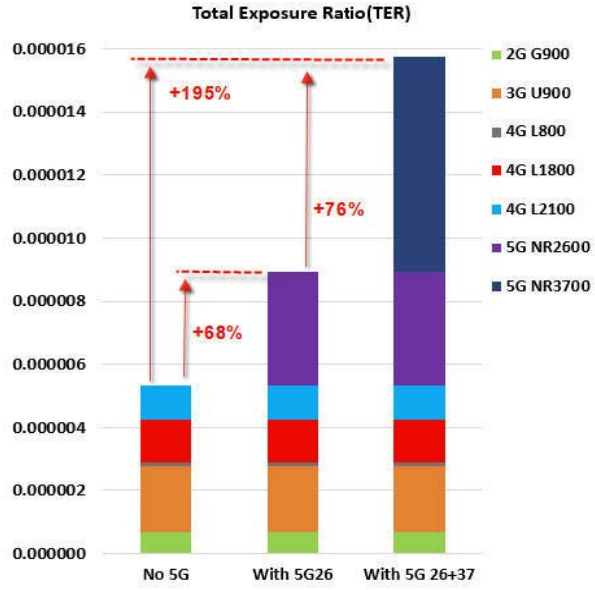


**FIGURE 20.** Site-2 (urban area) simulated an increase in the total exposure ratio TER due to the addition of 5G2600 and 5G3700.

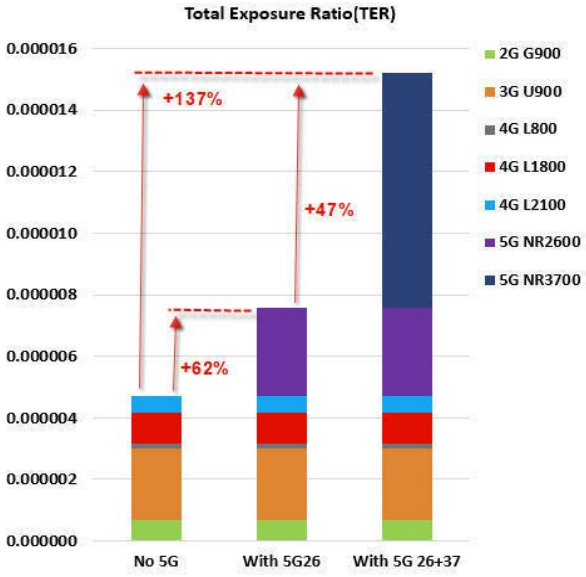


**FIGURE 21.** Site-3 (suburban area) simulated increments in the total exposure ratio TER due to the addition of 5G2600 and 5G3700.

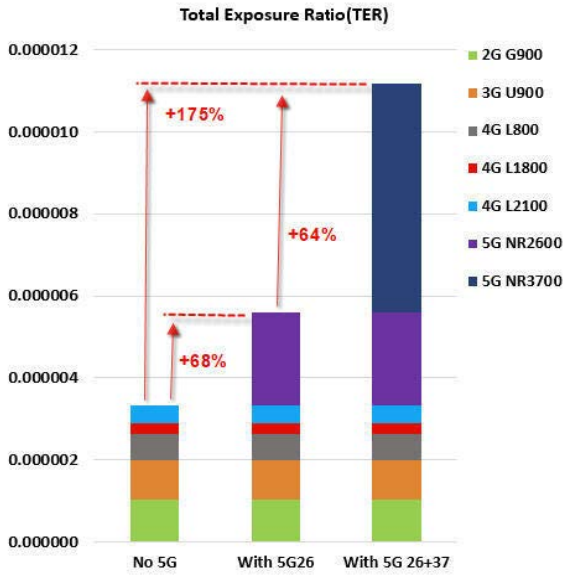


**FIGURE 22.** Site 4 (rural area) simulated an increase in the total exposure ratio TER due to the addition of 5G2600 and 5G3700.

focused on assessment for one technology, and in this work, the results present the accumulated TER.

Furthermore, the TER is analyzed to evaluate the contribution of each technology, which addresses and provides indications about forecast radiation increases for future incoming technologies and expansions. Therefore, we added a second technology of 5G NR at a frequency of 3.7 GHz, which is expected to be deployed at the same sites, including 64T/64R AAU with 180 watts, 100 MHz bandwidth, and the same antenna heights as other technologies.

The analysis of results for the dense area shows that TER is very low compared to the ICNIRP, with the highest being 0.0114% from the maximum limit. TER distribution FIGURE 19 shows that the addition of the first technology of 5G NR2600 (co-location with exiting 2G/3G/4G) raises the TER by 68% and the addition of the second technology of 5G NR 3700 raises the TER by 27%, so the total increase due to 5G technologies is 114%, which makes the 5G contribution to TER approximately 53%.

The urban area analysis also shows that TER is very low compared to the ICNIRP, with the highest being 0.0104% from the maximum limit. TER distribution FIGURE 20 shows that the addition of the first technology of 5G NR2600 (co-location with exiting 2G/3G/4G) raises the TER by 68%.

The addition of the second technology of 5G NR 3700 raises the TER by 76%; thus, the total increase due to both 5G technologies is 195%, which makes the 5G contribution to TER approximately 66%.

The suburban area analysis also shows that TER is very low compared to the ICNIRP, with the highest 0.098% from the maximum limit. TER distribution FIGURE 21 shows that the addition of the first technology of 5G NR2600 (co-location with exiting 2G/3G/4G) raises the TER by 62% and the addition of the second technology of 5G NR 3700 raises the TER by 47%; thus, the total increase due to 5G technologies is 137%, which makes the 5G contribution to TER approximately 53%.

The rural area analysis also shows that TER is very low compared to the ICNIRP, with the highest being 0.0066% from the maximum limit. TER distribution FIGURE 22 shows that the addition of the first technology of 5G NR2600 (co-location with exiting 2G/3G/4G) raises the TER by 68%. The addition of the second technology of 5G NR 3700 raises the TER by 64%; thus, the total increase due to both 5G technologies is 175%, which makes the 5G contribution to TER approximately 65%.

## IV. CONCLUSION

This study assessed the EMF exposure radiation for specific single sites in dense, urban, suburban, and rural areas considering multi-technology simultaneously operating and co-located at the same site, including 2G, 3G, 4G, IoT, and 5G. The assessment was performed through simulation tools using propagation models to predict the Rx levels, and the tool was calibrated using field measurements. The Rx level results were used to calculate the power densities at different distances from the sites, and the total exposure ratios were calculated from the power densities. The obtained results show that the power densities and total exposure ratios are low for the four area scenarios compared to the ICNIRP standard reference limits. Further studies will be conducted to investigate and assess the RF-EMF radiation exposure at the near field for single sites and groups of sites and surrounding sites in the whole area considering multi-technology and multi-operator coexistence. Additionally, further studies are required to investigate the exposure considering other factors, such as traffic load (system utilization), time-averaged power and spectral efficiency.

## REFERENCES

[1] A. Bajpai and A. Balodi, "Role of 6G networks: Use cases and research directions," in *Proc. IEEE Bengaluru Humanitarian Technol. Conf. (B-HTC)*, Oct. 2020, pp. 1–5, doi: 10.1109/B-HTC50970.2020.9298017.

[2] M. Z. Chowdhury, M. Shahjalal, S. Ahmed, and Y. M. Jang, "6G wireless communication systems: Applications, requirements, technologies, challenges, and research directions," *IEEE Open J. Commun. Soc.*, vol. 1, pp. 957–975, 2020, doi: 10.1109/OJCOMS.2020.3010270.

[3] W. J. Koh and S. M. Moochhala, "Non-ionizing EMF hazard in the 21th century," in *Proc. IEEE Int. Symp. Electromagn. Compat., IEEE Asia–Pacific Symp. Electromagn. Compat. (EMC/APEMC)*, May 2018, pp. 518–522, doi: 10.1109/ISEMC.2018.8393832.

[4] ICNIRP, "Guidelines for limiting exposure to electromagnetic fields (100 kHz to 300 GHz)," *Health Phys.*, vol. 118, no. 5, pp. 483–524, 2020.

[5] ICNIRP, "Guidelines for limiting exposure to time-varying electric, magnetic, and electromagnetic fields (up to 300 GHz)," *Health Phys.*, vol. 74, no. 4, pp. 494–522, 1998.

[6] *Evaluating Compliance With FCC Guidelines for Human Exposure to Radiofrequency Electromagnetic Fields*, F.O.B., FCC OET Bulletin 65, Federal Commun. Commission, Washington, DC, USA, 1997.

[7] W. El-Beaino, A. M. El-Hajj, and Z. Dawy, "On radio network planning for next generation 5G networks: A case study," in *Proc. Int. Conf. Commun., Signal Process., Their Appl. (ICCSPA)*, Feb. 2015, pp. 1–6, doi: 10.1109/ICCSPA.2015.7081315.

[8] L. Chiaraviglio, A. Elzanaty, and M.-S. Alouini, "Health risks associated with 5G exposure: A view from the communications engineering perspective," *IEEE Open J. Commun. Soc.*, vol. 2, pp. 2131–2179, 2021, doi: 10.1109/OJCOMS.2021.3106052.

[9] V. Markovic, "5G EMF exposure: Overview of recent research and safety standard updates," in *Proc. 15th Int. Conf. Adv. Technol., Syst. Services Telecommun. (TELSIKS)*, Oct. 2021, pp. 359–365, doi: 10.1109/TELSIKS52058.2021.9606262.

[10] M. S. Elbasheir, R. A. Saeed, A. A. Z. Ibrahim, S. Edam, F. Hashim, and S. M. E. Fadul, "A review of EMF radiation for 5G mobile communication systems," in *Proc. IEEE Asia–Pacific Conf. Appl. Electromagn. (APACE)*, Dec. 2021, pp. 1–6, doi: 10.1109/APACE53143.2021.9760689.

[11] M. S. Elbasheir, R. A. Saeed, and S. Edam, "5G base station deployment review for RF radiation," in *Proc. Int. Symp. Netw., Comput. Commun. (ISNCC)*, Oct. 2021, pp. 1–5, doi: 10.1109/ISNCC52172.2021.9615689.

[12] H. Malik, H. Pervaiz, M. M. Alam, M. Y. Le, A. Kuusik, and M. A. Imran, "Radio resource management scheme in NB-IoT systems," *IEEE Access*, vol. 6, pp. 15051–15064, 2018, doi: 10.1109/ACCESS.2018.2812299.

[13] *Technical Specification Group Radio Access Network; Evolved Universal Terrestrial Radio Access (E-UTRA); Services Provided by the Physical Layer (Release 16)*, document TS-36.302, 3GPP, 2020.

[14] Infovista. (2021). *TEMS Investigation—Mobile Network Testing Software*. [Online]. Available: https://www.infovista.com/tems/investigation

[15] L. Chiaraviglio, A. S. Cacciapuoti, G. Di Martino, M. Fiore, M. Montesano, D. Trucchi, and N. B. Melazzi, "Planning 5G networks under EMF constraints: State of the art and vision," *IEEE Access*, vol. 6, pp. 51021–51037, 2018, doi: 10.1109/ACCESS.2018.2868347.

[16] Infovista. (2021). *Planet—RF Planning Software*. [Online]. Available: https://www.infovista.com/5g-network/planet-rf-planning-software

[17] V. S. Anusha, G. K. Nithya, and S. N. Rao, "A comprehensive survey of electromagnetic propagation models," in *Proc. Int. Conf. Commun. Signal Process. (ICCSP)*, Apr. 2017, pp. 1457–1462, doi: 10.1109/ICCSP.2017.8286627.

[18] S. A. Siddiqui, N. Fatima, and A. Ahmad, "Comparative analysis of propagation path loss models in lte networks," in *Proc. Int. Conf. Power Electron., Control Automat. (ICPECA)*, Nov. 2019, pp. 1–3, doi: 10.1109/ICPECA47973.2019.8975464.

[19] *Study on 3D Channel Model for LTE*, document TR-36.873, 3GPP, 2018.

[20] T. Rappaport, Y. Xing, G. R. MacCartney, A. F. Molisch, E. Mellios, and J. Zhang, "Overview of millimeter wave communications for fifth-generation (5G) wireless networks-with a focus on propagation models," *IEEE Trans. Antennas Propag.*, vol. 65, no. 12, pp. 6213–6230, Dec. 2017, doi: 10.1109/TAP.2017.2734243.

[21] *Study on Channel Model for Frequencies From 0.5 to 100 GHz*, document TR-38.901, 3GPP, 2018.

[22] H. Tataria, K. Haneda, A. F. Molisch, M. Shafi, and F. Tufvesson, "Standardization of propagation models for terrestrial cellular systems: A historical perspective," *Int. J. Wireless Inf. Netw.*, vol. 28, no. 1, pp. 20–44, Mar. 2021.

[23] A.-K. Lee, S.-B. Jeon, and H.-D. Choi, "EMF levels in 5G new radio environment in Seoul, Korea," *IEEE Access*, vol. 9, pp. 19716–19722, 2021, doi: 10.1109/ACCESS.2021.3054363.

[24] A. Gati, E. Conil, M.-F. Wong, and J. Wiart, "Duality between uplink local and downlink whole-body exposures in operating networks," *IEEE Trans. Electromagn. Compat.*, vol. 52, no. 4, pp. 829–836, Nov. 2010, doi: 10.1109/TEMC.2010.2066978.

[25] GSMA. (2019). *Public Policy 2019*. [Online]. Available: https://www.gsma.com/publicpolicy/emf-and-health/emf-policy

[26] C. Phillips, D. Sicker, and D. Grunwald, "Bounding the error of path loss models," in *Proc. IEEE Int. Symp. Dyn. Spectr. Access Netw. (DySPAN)*, May 2011, pp. 71–82, doi: 10.1109/DYSPAN.2011.5936271.

[27] D. G. Lopez, M. Ignatenko, and D. S. Filipovic, "Eigenmode prediction of high RF exposure frequency region inside vehicles," *IEEE Trans. Electromagn. Compat.*, vol. 59, no. 1, pp. 43–47, Feb. 2017, doi: 10.1109/TEMC.2016.2593023.
[28] U. T. Virk, K. Haneda, V.-M. Kolmonen, P. Vainikainen, and Y. Kaipainen, "Characterization of vehicle penetration loss at wireless communication frequencies," in *Proc. 8th Eur. Conf. Antennas Propag. (EuCAP)*, Apr. 2014, pp. 234–238, doi: 10.1109/EuCAP.2014.6901733.
[29] W. H. Bailey, B. R. T. Cotts, and P. J. Dopart, "Wireless 5G radiofrequency technology—An overview of small cell exposures, standards and science," *IEEE Access*, vol. 8, pp. 140792–140797, 2020, doi: 10.1109/ACCESS.2020.3010677.
[30] R. Ramirez-Vazquez, I. Escobar, A. Thielens, and E. Arribas, "Measurements and analysis of personal exposure to radiofrequency electromagnetic fields at outdoor and indoor school buildings: A case study at a Spanish school," *IEEE Access*, vol. 8, pp. 195692–195702, 2020, doi: 10.1109/ACCESS.2020.3033800.
[31] T. Rumeng, S. Ying, W. Tong, and Z. Wentao, "Electromagnetic field safety compliance assessments for 5G wireless networks," in *Proc. IEEE Int. Symp. Electromagn. Compat. Signal/Power Integrity (EMCSI)*, Jul. 2020, pp. 659–662, doi: 10.1109/EMCSI38923.2020.9191518.
[32] B. Thors, A. Furuskär, D. Colombi, and C. Törnevik, "Time-averaged realistic maximum power levels for the assessment of radio frequency exposure for 5G radio base stations using massive MIMO," *IEEE Access*, vol. 5, pp. 19711–19719, 2017, doi: 10.1109/ACCESS.2017.2753459.
[33] S. Aerts, L. Verloock, M. Van Den Bossche, D. Colombi, L. Martens, C. Törnevik, and W. Joseph, "*In-situ* measurement methodology for the assessment of 5G NR massive MIMO base station exposure at sub-6 GHz frequencies," *IEEE Access*, vol. 7, pp. 184658–184667, 2019, doi: 10.1109/ACCESS.2019.2961225.
[34] A. Pathak and A. Jangid, "Measurement and impact assessment of radio frequency electromagnetic fields in Dayalbagh educational institute," in *Proc. IEEE 9th Power India Int. Conf. (PIICON)*, Feb. 2020, pp. 1–5, doi: 10.1109/PIICON49524.2020.9113039.
[35] D. Colombi, P. Joshi, B. Xu, F. Ghasemifard, V. Narasaraju, and C. Törnevik, "Analysis of the actual power and EMF exposure from base stations in a commercial 5G network," *Appl. Sci.*, vol. 10, no. 15, p. 5280, Jul. 2020.
[36] S. Q. Wali, A. Sali, J. K. Allami, and A. F. Osman, "RF-EMF exposure measurement for 5G over mm-wave base station with MIMO antenna," *IEEE Access*, vol. 10, pp. 9048–9058, 2022, doi: 10.1109/ACCESS.2022.3143805.
[37] M. Celaya-Echarri, L. Azpilicueta, J. Karpowicz, V. Ramos, P. Lopez-Iturri, and F. Falcone, "From 2G to 5G spatial modeling of personal RF-EMF exposure within urban public trams," *IEEE Access*, vol. 8, pp. 100930–100947, 2020, doi: 10.1109/ACCESS.2020.2997254.
[38] M. Velghe, S. Aerts, L. Martens, W. Joseph, and A. Thielens, "Protocol for personal RF-EMF exposure measurement studies in 5th generation telecommunication networks," *Environ. Health*, vol. 20, no. 1, pp. 1–10, Dec. 2021.
[39] M. Velghe, S. Shikhantsov, E. Tanghe, L. Martens, W. Joseph, and A. Thielens, "Exposure to RF-EMF hotspots induced by maximum ratio field combining in 5th generation networks," in *Proc. Joint Annu. Meeting Bioelectromagnetics Soc. Eur. BioElectromagnetics Assoc. (BioEM)*, 2020, pp. 380–384.
[40] S. Aerts, W. Joseph, M. Maslanyj, D. Addison, T. Mee, L. Colussi, J. Kamer, and J. Bolte, "Prediction of RF-EMF exposure levels in large outdoor areas through car-mounted measurements on the enveloping roads," *Environ. Int.*, vol. 94, pp. 482–488, Sep. 2016.

**MOHAMMED S. ELBASHEIR** received the B.Sc. degree in electrical engineering and the M.Sc. degree in communication engineering from the University of Khartoum, Sudan, in 2006. He is currently pursuing the Ph.D. degree in wireless communication with the School of Electronic Engineering, Sudan University of Science and Technology, Khartoum, Sudan. From 1998 to 2005, he worked as a Planning and Optimization Engineer at Etisalat Corporation, United Arab Emirates. Since 2006, he has been working as the Senior Director of mobile radio access network planning and design with Etihad Etisal Company (Mobily), Saudi Arabia.

**RASHID A. SAEED** received the Ph.D. degree in communications and network engineering from the Universiti Putra Malaysia (UPM). He was a Senior Researcher with Telekom Malaysia$^{TM}$ Research and Development (TMRND) and MIMOS. He is currently a Professor with the Computer Engineering Department, Taif University, Saudi Arabia. He is also working with the School of Electronics Engineering, Sudan University of Science and Technology (SUST). He published more than 150 research papers, books, and book chapters on wireless communications and networking in peer-reviewed academic journals and conferences. His research interests include computer networks, cognitive computing, computer engineering, wireless broadband, and WiMAX femtocell. He is successfully awarded three U.S. patents in these areas. He supervised more than 50 M.Sc./Ph.D. students. He is a member of IEM (I.E.M), SigmaXi, and SEC.

**SALAHELDIN EDAM** received the B.Sc. degree in electronics engineering from the Sudan University of Science and Technology (SUST), the Post Graduate Diploma (APGD) degree in 'advanced information technology (advanced networking and telecommunication), the M.Sc. degree in information technology (computer network systems) from the SUST, and the Ph.D. degree in engineering in communications and information systems from the Beijing University of Posts and Telecommunications (BUPT). He was an Engineer at Sudan Telecommunication Company (Sudatel). He is currently an Assistant Professor with the School of Electronics Engineering, SUST. He supervised many M.Sc. students in addition to co-supervisor for many Ph.D. students. He published many research papers in journals and conferences. His research interests include wireless communications, software-defined networking, the IoT, and computer network systems.